IJST, Transactions of Mechanical Engineering, Vol. 38, No. M1, pp 9-23
Printed in The Islamic Republic of Iran, 2014

COMPARISON BETWEEN TWO METHODS FOR ENHANCING HEAT TRANSFER IN SEPARATED CONVECTION FLOWS-SECOND LAW ANALYSIS*

S. A. GANDJALIKHAN NASSAB[1**], A. BAHRAMI[2], M. M. KESHTKAR[3] AND M. H. SAFFARIPOUR[4]

[1,2,4]Dept. of Mechanical Engineering, Shahid Bahonar University, Kerman, I. R. of Iran
Email: ganji110@uk.ac.ir
[3]Dept. of Mechanical Engineering, Kerman Branch of Islamic Azad University, I. R. of Iran

Abstract– In the present work, a laminar forced convection flow over a backward-facing step (BFS) in a duct is investigated. This study concerns the practical application of entropy generation analysis in separated convective flow for the first time. Two different methods, (i) attaching a baffle to the channel top wall and (ii) employing suction for enhancing heat transfer performance, are compared by the second law criteria. Entropy generation in the flow domain which indicates the amount of irreversibilities in convective flow is computed numerically. Heat transfer and viscous dissipation are the two sources of entropy generation in convective flow. The set of governing equations defining conservations of mass, momentum and energy are solved numerically to calculate velocity and temperature profiles which are needed for estimating entropy generation. The SIMPLE algorithm is used to resolve the pressure-velocity coupling. Numerical expressions, in terms of entropy generation number (*Ns*) and Nusselt number (*Nu*) are derived in dimensionless forms. The total entropy generation is also calculated in different case studies for comparing the amount of irreversibilities. Numerical results revealed that using baffles and permeable walls with suction have considerable effects in enhancing heat transfer but the presence of baffle produces more irreversibilities than the suction technique.

Keywords– Entropy generation, suction, baffle, backward facing step, forced convection, irreversibility

1. INTRODUCTION

Forced convection in channels with sudden expansion in flow geometry is widely encountered in engineering applications such as in the cooling of electronic systems, power generating equipment, combustors and compact heat exchangers. One of the primary objectives in the design of any energy system is to conserve the useful energy supplied for a certain process to take place. The irreversibilities associated within the process components destroy the useful energy and decrease the system performance. The optimal second law design criteria depends on the minimization of entropy generation encountered in fluid and heat transfer processes in energy systems [1].

In many cases of convection flows, it is desirable to enhance heat transfer over heating surfaces. There are many techniques for this purpose such as installing wall baffle mounted for directing the flow toward the heating surface and also using permeable surfaces with bleeding. In the present work, these two methods are compared by applying the second law analysis and computing the entropy generation. Recently, entropy generation analysis has been extensively applied in many fluid flows with heat transfer in different geometries. Heat transfer and viscous dissipation are the only sources of entropy generation in forced convective fluid flows. In a recent study, Ko and Wu [2] analyzed the entropy generation induced

*Received by the editors February 8, 2012; Accepted August 31, 2013.
**Corresponding author

by turbulent forced convection in a curved rectangular duct with external heating by numerical methods. The flow features, including the secondary flow motions, the distribution of local entropy generation as well as the overall entropy generation in the whole flow fields, were analyzed. The results showed that the entropy generation induced by the frictional irreversibility concentrates within the regions adjacent to the solid surfaces. Calculation of entropy generation in the flow over forward or backward facing steps has many engineering applications, such as computation of irreversibility and energy loss in separated regions encountered for flow over gas turbine blades and combustion chambers. Recently, in a paper by Bahrami and Gandjalikhan Nassab [3], entropy generation in laminar forced convection flow over a forward facing step in a duct was analyzed by CFD method. Momentum and energy equations were solved numerically in the Cartesian coordinate system using the SIMPLE algorithm. Numerical expressions in terms of entropy generation number and Nusselt number were derived in dimensionless form using velocity and temperature profiles. Also, the regions with small and high rates of irreversibility were distinguished in that work. There are a few studies in which the analysis of entropy generation due to forced convective flow over a BFS has been conducted (Abu Nada [4, 5]). In those studies, the set of governing equations consisting of conservation of mass, momentum and energy were solved numerically by CFD method and the computed velocity and temperature field were used to solve the entropy generation equations.

On the other hand, the problems of fluid flow in ducts and channels with permeable walls have received much attention from investigators due to increasing use of suction and injection in modern technology. A particularly relevant example is that of turbine blades of the modern aircraft engines, which are currently cooled by the passage of relatively cool air tapped from the compressor, either through hollow blades or through span-wise holes drilled in solid blades. There are several studies about fluid flows through ducts and channels with bleeding (Duwez and Wheeler [6]; Mehta and Jain [7]; Erdogan and Imrak [8]). As a common important result in those studies, it was reported that the suction and blowing have considerable effects on the rate of heating or cooling in thermal systems. Recently, investigation of entropy generation in a flow over a BFS under bleeding condition (suction/blowing) was done by Abu-Nada [9]. The set of governing equations were solved by CFD (Computational Fluid Dynamics) method and the distributions of entropy generation number on solid surfaces at different conditions were calculated. Moreover, the effects of bleed coefficient for both blowing and suction on the entropy generation number were studied. It was found that blowing increases the amount of entropy generation in the convection flow, whereas suction reduces it.

In all of the above research works, the separated convection flows over backward or forward facing steps were under study. In many practical applications, separated convection flow over recess including both backward and forward steps takes place. This type of convection flow was studied by Atashafrooz and Gandjalikhan Nassab [10] with the presence of radiating heat transfer. For this purpose, the set of governing equations was solved numerically where the radiative term in the energy equation was calculated by the discrete ordinate method. Finally, the effects of several parameters on thermal behavior of this type of thermal system were carried out.

The optimal design of new thermal systems indicates the importance of finding effective methods for enhancing heat transfer. Using baffles is an appropriate way for this purpose. Numerical simulations by Tsay et al. [11] revealed that the average Nusselt number on the heated wall can be enhanced by placing a baffle in the two-dimensional backward facing step flow. In a recent work by Nie et al. [12] about convection over BFS, the effect of baffle on convection coefficient in a three-dimensional convection flow was studied. Numerical solution of the continuity, momentum and energy equations together with the boundary conditions was performed by utilizing the SIMPLE algorithm for the pressure correction in the iteration procedure. It was revealed that a baffle mounted onto the upper wall significantly increases the

magnitude of maximum Nusselt number at the stepped wall. In that study, the effects of baffle location and its height on flow and heat transfer distributions were determined.

As it is mentioned in the above research works, using baffles and also employing bleeding on heated surface leads to enhancing the rate of convection heat transfer, but choosing the best way from these alternatives remains as another research study which is done here based on the second law analysis and calculating entropy generation that can show the rate of irreversibilities. Therefore, in the present work, two different methods for enhancing convection heat transfer in a forced convection separated flow over an inclined BFS in a duct are compared by applying the second law analysis. Then the best way is distinguished in which more enhancing convection heat transfer occures with less irreversibility as a result of applying this technique. To the best of the authors' knowledge, there are no similar studies in the published literature. This fact, along with the realization that such flow geometry appears regularly in many industrial heat transfer devices, such as electronic cooling, heat exchanger and others, motivated the present research. Toward this end, the set of governing equations consisting of conservation of mass, momentum and energy are solved by the CFD method. For having more generality, the step is considered to be inclined. Consequently, in numerical solution of the governing equations in the Cartesian coordinate system, the blocked-off method is employed for simulation of the inclined boundary in the (x, y) plane. By this method, the amount of viscosity for all grid points inside the solid region is considered too large for having zero fluid velocity in that domain. From the numerical results, the amounts of entropy generation and convection coefficient under the presence of wall mounted baffle and permeable wall with bleeding are calculated in the flow domain and compared to each other.

2. THEORY

a) Governing equations

In order to determine the amount of entropy generation in the forced convection flow as indicated in Fig.1, the velocity and temperature distributions are primarily needed. The set of governing equations can be written in the Cartesian coordinate system (x, y) as follows:

$$\frac{\partial U}{\partial X}+\frac{\partial V}{\partial Y}=0 \tag{1}$$

$$\frac{\partial}{\partial X}\left(U^2-\frac{1}{\mathrm{Re}}\frac{\partial U}{\partial X}\right)+\frac{\partial}{\partial Y}\left(UV-\frac{1}{\mathrm{Re}}\frac{\partial U}{\partial Y}\right)=-\frac{\partial P}{\partial X} \tag{2}$$

$$\frac{\partial}{\partial X}\left(UV-\frac{1}{\mathrm{Re}}\frac{\partial V}{\partial X}\right)+\frac{\partial}{\partial Y}\left(V^2-\frac{1}{\mathrm{Re}}\frac{\partial V}{\partial Y}\right)=-\frac{\partial P}{\partial Y} \tag{3}$$

$$\frac{\partial}{\partial \mathrm{X}}\left(\mathrm{U}\Theta-\frac{1}{\mathrm{Pe}}\frac{\partial \Theta}{\partial \mathrm{X}}\right)+\frac{\partial}{\partial \mathrm{Y}}\left(\mathrm{V}\Theta-\frac{1}{\mathrm{Pe}}\frac{\partial \Theta}{\partial \mathrm{Y}}\right)=\phi \tag{4}$$

In the above equations, the following dimensionless groups are used:

$$(X,Y)=\left(\frac{x}{D_H},\frac{y}{D_H}\right),\ (U,V)=\left(\frac{u}{V_0},\frac{v}{V_0}\right),\ P=\frac{p}{\rho V_0^2},\ \mathrm{Re}=\frac{\rho V_0 D_H}{\mu},\ \Theta=\frac{T-T_c}{T_h-T_c}$$

$$Pe = Re.\ Pr$$

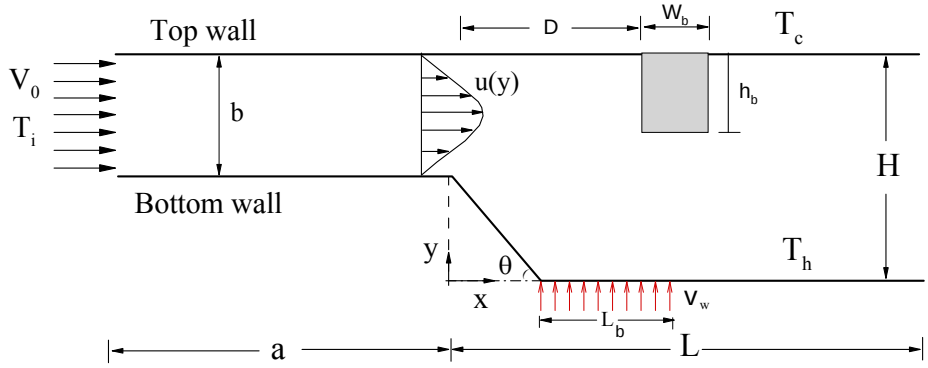

Fig. 1. Physical model and computational domain

In these dimensionless parameters, D_H is the hydraulic diameter which is equal to 2b, V_0 is the fluid velocity at the duct's inlet section and *Pr* is the prandtl number. It should be mentioned that the right hand side of the energy equation is the viscous dissipation which must be taken into account in fluid flows with high Brinkman number.

In the present study, the values of all parameters needed in the computations except those used for validating numerical results, are listed in Table. 1.

Table 1. The values of parameters used in the computations

Parameter	θ	L_b	a	b	L	W_b	h_b
Value	60^0	10H	5H	0.5H	25H	0.5H	0.5H

b) Entropy generation

As it was noted before, the entropy generation in a convection flow is due to the irreversibilities caused by viscous friction and heat transfer. The entropy generation in dimensionless form is given as follows: (for a detailed derivation see [1])

$$Ns = \Psi \times \left\{ 2 \times \left[\left(\frac{\partial U}{\partial X} \right)^2 + \left(\frac{\partial V}{\partial Y} \right)^2 \right] + \left[\left(\frac{\partial U}{\partial Y} \right) + \left(\frac{\partial V}{\partial X} \right) \right]^2 \right\} + \left[\left(\frac{\partial \Theta}{\partial X} \right)^2 + \left(\frac{\partial \Theta}{\partial Y} \right)^2 \right] \tag{5}$$

The following dimensionless quantities are defined:

$$Ns = \frac{s''_{gen} D_h^{\,2}}{k\tau^2} \quad , \quad \tau = \frac{T_h - T_c}{T_c} \quad , \quad Br = \frac{\mu V_0^2}{k(T_h - T_c)} \quad , \quad \Psi = \frac{Br}{\tau}$$

where *Ns* is the entropy generation number, S''_{gen} the volume rate of entropy generation, *Br* the Brinkman number and τ is the non-dimensional temperature difference. In Eq. (5), the first term represents the entropy generation due to the fluid viscous effect (Ns_{visc}), while the second term represents the entropy generation due to the heat transfer (Ns_{cond}).

c) Regular grid with blocked-off region

In many cases, a computer program written for a regular grid can be improved to handle an irregularly shaped computational domain. This can be done by rendering inactive some of the control volumes of the regular grid so that the remaining active control volumes form the desired irregular domain with complex boundary. Figure 2 shows an example of a discretized computational with blocked-off

region in a regular grid. Since in the present study, the set of governing equations are solved numerically in the Cartesian coordinate system, the surface of inclined boundary is approximated by a series of rectangular steps. It is obvious that using fine grids in the interface region between active and inactive zones causes an approximated boundary which is more similar to the true boundary.

According to the blocked-off technique, known values of the dependent variables must be established in all inactive control volumes. If the inactive region represents a stationary solid boundary as in the case, the velocity components in that region must be equal to zero. In the present computations, zero velocity in the inactive zone is employed by use of a very large viscosity for grid points in that zone with a zero value of velocity on the nominal boundaries.

d) Boundary conditions

Equations (1) to (4) are solved by considering appropriate boundary conditions. For the fluid flow problem, no-slip condition is applied on solid boundaries. Besides, at the inlet section, slug flow with velocity V_0 is considered and at the outlet section, zero velocity gradient in axial direction is employed for both u- and v- velocity components.

For the thermal problem, the top wall and bottom wall including the step are kept at constant temperature T_c and T_h, respectively. Besides, at the inlet section, a uniform temperature T_i is assumed and zero temperature gradient in axial direction is employed at the outlet section.

3. SOLUTION PROCEDURE

Finite difference forms of the partial differential Eqs. (1) to (4) are obtained by integrating them over an elemental cell volume with staggered control volumes for the x- and y-velocity components. Other variables of interest are computed at the grid nodes. The hybrid method is used for approximating the convective terms in the momentum equations. By this technique, the finite difference form of the governing equations for any dependent variable Φ can be written in the following common form:

$$AP.\Phi_P + AN.\Phi_N + AS.\Phi_S + AE.\Phi_E + AW.\Phi_W = S_\Phi \tag{6}$$

The discretized forms of the governing equations are numerically solved by the SIMPLE algorithm of Patankar and Spalding [13]. Numerical solutions are obtained iteratively by the line-by-line method, such that iterations are terminated when the sum of the absolute residuals is less than 10^{-4} for each equation. Numerical calculations are performed by writing a computer program in FORTRAN. As a result of grid tests for obtaining the grid-independent solution, an optimum grid of 400×125 with clustering near the solid surfaces is determined in the x- and y- directions. A schematic of grid points in the computational domain is shown in Fig. 2. After computing the flow and temperature distributions, Eq. (6) is solved for the entropy generation number at each grid point in the flow domain. Total entropy generation through the flow domain which shows the amount of irreversibilities in the convection flow is also calculated by the following equation:

$$Ns_{Total} = \int_{\forall} Ns(X,Y)d\forall \tag{7}$$

where in the present two-dimensional case, the volume of computational domain per unit length perpendicular to the (x, y) plane, dented by $\forall$, is equal to the area of the computational zone.

Besides, the distributions of Nusselt number, $Nu = h D_H / k$, along the heated wall is calculated at different conditions. In the definition of Nusselt number, h is the convection coefficient that can be obtained by:

$$h = \frac{\left[-k \frac{\partial T}{\partial y} \right]_{wall}}{T_w - T_m} \tag{8}$$

In which T_m is the fluid mean bulk temperature at each axial section.

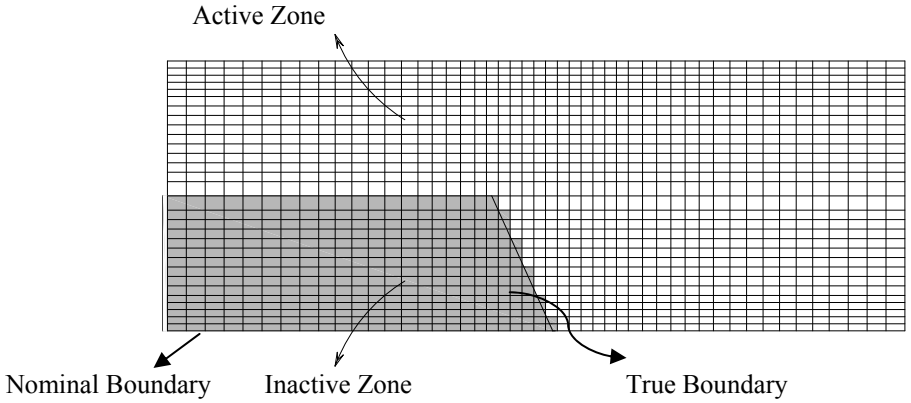

Fig. 2. Blocked-off region in a regular grid

4. RESULTS AND DISCUSSION

Since, there is no experimental data about entropy generation in convection flow adjacent to BFS, comparison with experiment is made for flow field computation. Experimental study of convection flow over a backward facing step in a duct with *ER*=2 and $\theta = 90^o$ was carried out by Armaly et al. [14] and the variation of reattachment length with the Reynolds number is shown in Fig. 3. This figure shows that the extent of recirculation region adjacent to step increases with increase in Re such that the reattachment point moves downwards. However, Fig. 3 indicates a good agreement among the present numerical results and the experiments.

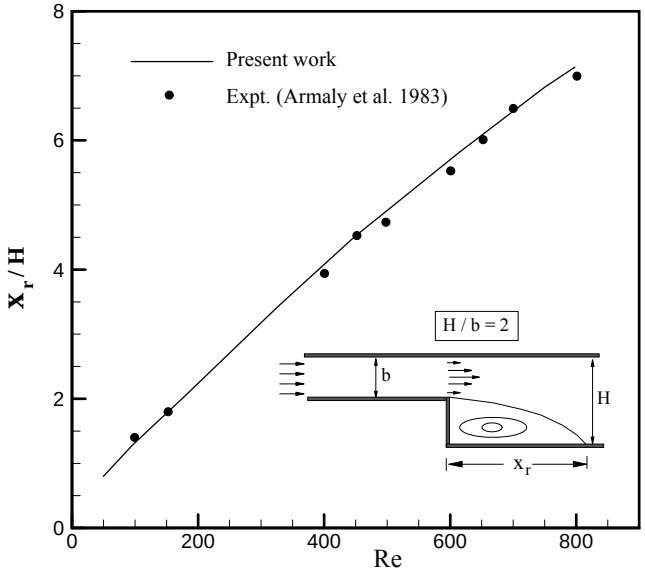

Fig. 3. Variation of reattachment length with *Re* , $\theta = 90^{\circ}$

To validate the computation of entropy generation in convection flow, numerical result for a test case is compared with the theoretical finding by Abu-Nada [9] in Fig. 4. In this test case, a laminar forced

convection flow over a vertical backward facing step in a duct with bleeding on the bottom wall in the region $0 \le x \le 10H$ is analyzed. The variations of entropy generation number *Ns* along the bottom wall for two different bleed coefficients ($\sigma = 0$ and $\sigma = 0.005$ corresponding to impermeable and permeable walls with blowing) are shown in Fig. 3 with *Re*= 400 and $\theta = 90^o$. It is seen that the minimum value of *Ns* occurs directly at x=0 at the bottom step corner, where the fluid has no motion. Also, Fig.4 shows that the maximum value of *Ns* occurs inside the recirculation zone and then drops sharply to a very low value at the reattachment point. This behavior can be explained by noting that after flow separation, the vortices increase dramatically inside the recirculation region that causes the maximum value of *Ns* to take place in this zone. Besides, at the reattachment point no shear stresses have occurred and the entropy generation is totally due to the conduction. After the reattachment point, *Ns* increases to a constant value far away from the step where fully developed condition is achieved. It is seen from Fig. 4 that blowing reduces the value of entropy generation number which is due to the decreased temperature and velocity gradients for the case of fluid injection. However, according to Fig. 4, the general agreement between the present results with the theoretical finding by Abu-Nada [9] is quite good and the values of minimum and maximum entropy generation numbers and their predicted locations are reasonably close to each other.

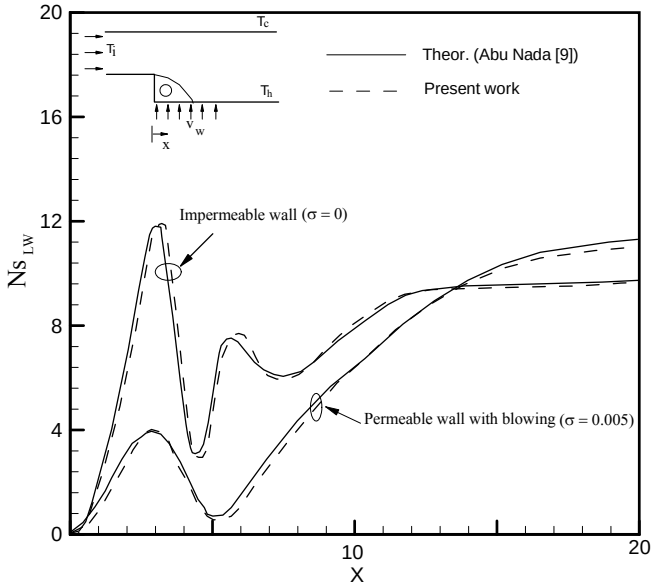

Fig. 4. Variation of entropy generation number along the bottom wall
Re=400, $\theta = 90^\circ$

Furthermore, the present numerical implementation about thermal behavior of the convection flow is validated by reproducing the theoretical results of other investigators. In the related test case, the results of Nusselt number on the bottom wall in convection flow over a BFS with baffle are compared with those presented by Nie et al. [12] In that work, the BFS was considered to be vertical to the stepped wall of the duct with *ER*=2. The bottom wall is heated with constant heat flux, while the top wall is maintained as being thermally adiabatic. It should be noted that in solving the governing equations for this test case, the same values for parameters which were used by Nie et al. [12] are considered in the present computations. Figure 5 shows the variation of Nusselt number along the bottom wall of the duct after the step. It is seen that the value of maximum Nusselt number increases due to the baffle effect. For instance, the maximum Nusselt number for D/H=1 is about three times that of $D/H \to \infty$ (without baffle). Also, the location of $Nu_{\max}$ moves downstream as the baffle moves along the streamwise direction. Figure 5 shows that the general agreement between the present results with the theoretical findings by Nie et al. [12] is quite good

and the values of minimum and maximum Nusselt numbers and their predicted locations are reasonably close to each other.

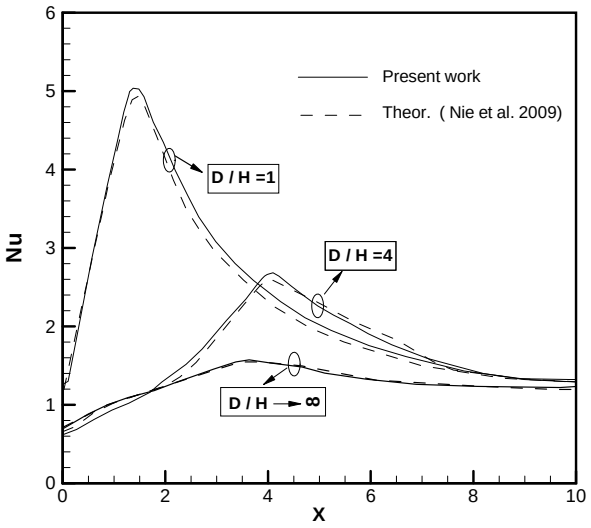

Fig. 5. Distribution of Nusselt number on the bottom wall at two different baffle locations, *Re*=343, $\theta = 90^{\circ}$

The following research results are presented for air flow adjacent to a backward facing step with the inclined angle $\theta = 60^{\circ}$ in a duct at Reynolds number equal to 400. In the computations, Prandtl number is kept constant at 0.71 to guarantee constant fluid physical properties for moderate and small values of the temperature difference $(T_h - T_c)$. According to the physical domain shown in Fig. 1, the expansion ratio (*ER*=H/b) is set equal to 2. Besides, the values of non-dimensional temperatures for the bottom wall (including the step), top wall and inlet fluid are set equal to 1, 0 and 0.7, respectively. Also, the numerical results are obtained for the non-dimensional temperature difference equal to 0.15, while the Brinkman number is equal to 10^{-5}. The computational domain in the x-direction has a length of 30H, while the distance between the inlet section and step is depicted by a value equal to 5H to ensure fully developed condition for velocity and temperature distributions before the step. Also, in the computations it is assumed that the permeable wall with bleeding has a length of $L_b = 10H$ (Fig. 1). It is worth mentioning that both negative and positive values of the bleed coefficient, σ, are used in the present work corresponding to suction and blowing, respectively.

First, in order to demonstrate the effect of baffle on the flow pattern, the streamlines are plotted in Fig. 6 for a wall mounted baffle with D/H=1, $W_b = h_b = H/2$. The effects of step and baffle on the flow are clearly seen from the curvatures of streamlines and separated regions. Figure 6 shows that five different recirculation zones are encountered for *Re*=400 in the flow domain. The primary recirculation region on the bottom wall occurs adjacent to the step upstream the baffle and the secondary one takes place on the bottom wall downstream the baffle, whereas three other recirculation zones occur adjacent to the baffle surface.

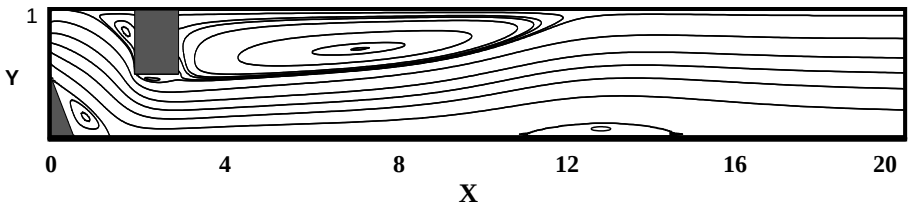

Fig. 6. Streamlines in flow over inclined step in a duct with a wall mounted baffle with $D/H = 1, W_b = h_b = H/2, \mathrm{Re} = 400$

To show the effect of bleeding on flow distribution, the streamlines downstream the step are plotted in Fig. 7 at three different bleeding coefficients including both suction and blowing. Figure 7 shows a recirculation zone adjacent to the bottom wall downstream the step for all values of the bleeding coefficient. The effect of bleeding on the fluid flow is clearly seen, such that in the case of suction, the reattachment point in the primary recirculation and the secondary recirculation zone also appears on the top wall after the step.

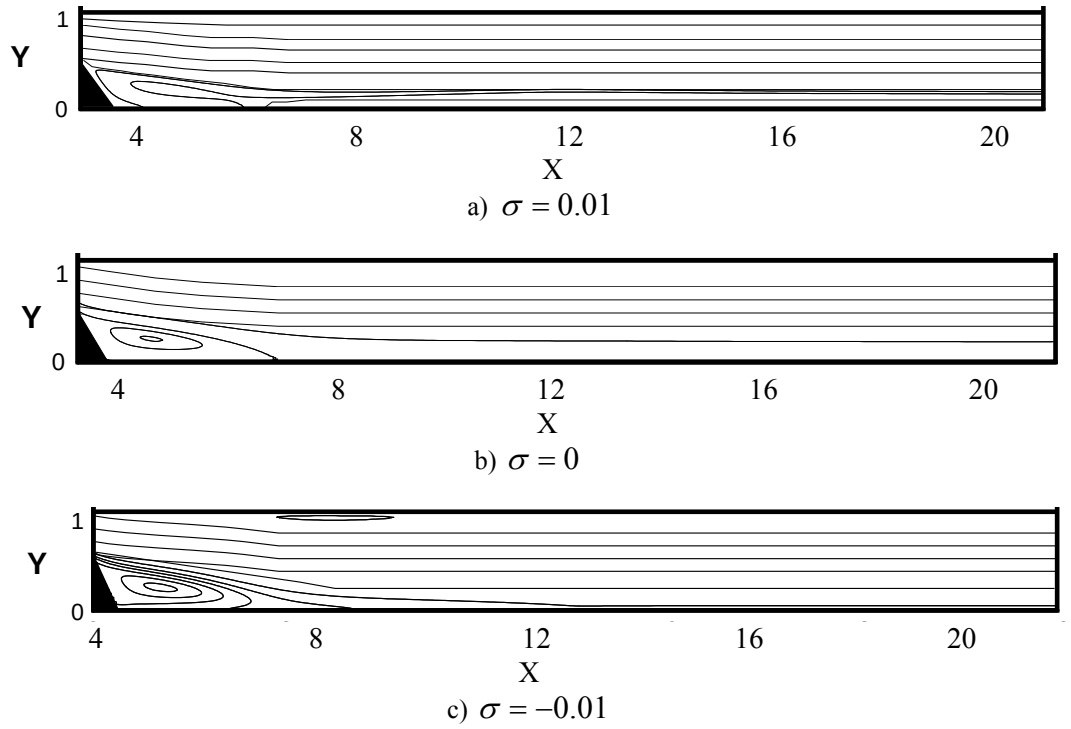

Fig. 7. Streamlines in flow over inclined step in a duct with three different values of the bleeding coefficient

In Fig. 8, the streamlines in the duct under the simultaneous presence of baffle and permeable wall with suction are plotted. If one compares this figure with the streamlines shown in Fig. 6, it can be seen that the flow distribution is considerably affected by the suction such that the separated region adjacent to the upper wall after the baffle enlarges and also the secondary recirculation zone on the bottom wall disappears by the suction process.

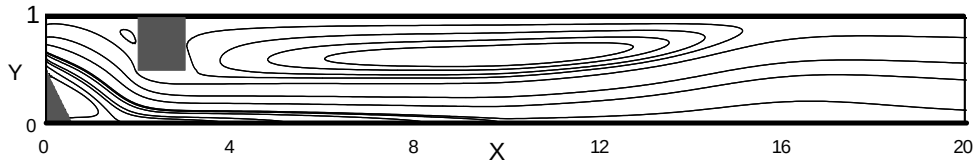

Fig. 8. Streamlines in flow over inclined step in a duct with a wall mounted baffle under the presence of suction, $\sigma = -0.03$

Since the main task of the present study is to compare two methods (using baffle and permeable wall with bleeding) for enhancing heat transfer from second law analysis, the following results show the effect of these factors on convection coefficient and also on entropy generation in the flow domain.

To study the effect of bleeding on the convection coefficient over the heated wall, the variations of Nusselt number defined as $Nu = h D_H / k$ along the bottom wall at three different bleeding coefficients are plotted in Fig. 9a. It is seen that the minimum value of *Nu* occurs on the bottom wall adjacent to the step corner where the fluid has no motion. Then the maximum value of Nusselt number takes place at the reattachment point after which *Nu* approaches to a constant value where flow becomes fully developed.

This behavior is due to this fact that flow reattaching on the heated wall increases the value of temperature gradient and then the rate of convection heat transfer. It is found in Fig. 9a that suction increases the value of Nusselt number along the bottom wall. This is related to the increased temperature and velocity gradients for the case of suction compared to that of blowing. Based on Fig. 9a, numerical computation of the average Nusselt number in the range of $0 \le x \le 10H$ indicate about 50% increase in the value of this parameter by the suction with bleeding coefficient $\sigma = -0.01$. For this test case, the variations of entropy generation number *Ns* along the bottom wall are plotted in Fig. 9b. It is seen that for all values of the bleeding coefficient, the maximum value of *Ns* occurs inside the recirculation zone and then drops sharply to a very low value at the point of reattachment. This behavior, which was also seen in Fig. 4, can be explained as, after flow separation, the vortices inside the recirculation region increase the value of *Ns* in this zone. Besides, at the reattachment point there are no shear stresses and the entropy generation is totally due to the conduction. It is found in Fig. 9b that suction increases the value of *Ns* and blowing reduces the entropy generation number. This is related to the increased temperature and velocity gradients for the case of suction in comparison to blowing. If one focuses on the entropy generation curves in the vicinity of x=0, it is seen that *Ns* decreases along the projected area of the step and becomes zero on the bottom wall coinciding with the step corner. This is due to the no-slip velocity and zero velocity gradient at this point.

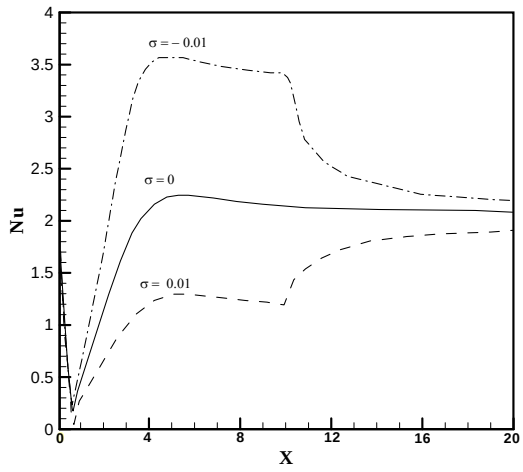

a) Distribution of Nusselt number along the bottom wall

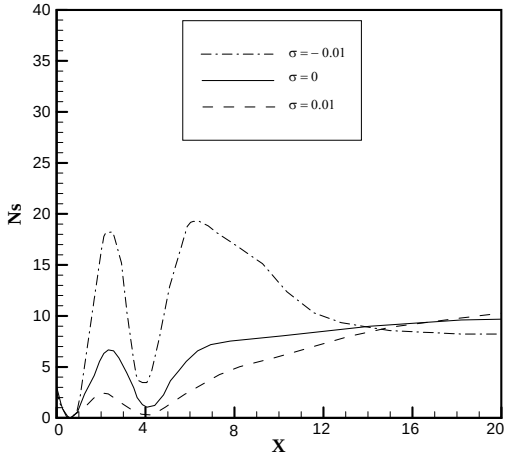

b) Distribution of entropy generation number along the bottom wall

Fig. 9. Effect of bleeding on the distributions of Nusselt number and entropy generation number along the bottom wall (without baffle)

In a similar manner, the effects of baffle on *Nu* and *Ns* distributions along the bottom wall are shown in Fig. 10. Variations of Nusselt number on the bottom wall at different locations of the baffle are plotted in Fig. 10a. It is seen that the maximum Nusselt number takes place just below the baffle with a value that is much greater than that without baffle ($D/H \to \infty$). This is because the fluid is effectively directed by the baffle toward the bottom wall that leads to a considerable increase in the convection coefficient, and the maximum Nusselt number takes place just below the baffle. Besides, it is seen from Fig. 10a that the maximum Nusselt number increases as the baffle moves toward the BFS, because the existence of baffle near the step directs the fluid flow toward the heated wall more effectively. Numerical computations of this figure indicate about 50% increase in the value of the average Nusselt number in the range of $0 \le x \le 10H$ by the baffle, such that the amount of increase in $Nu_{average}$ by the baffle is nearly equal to that obtained with suction ($\sigma = -0.01$).

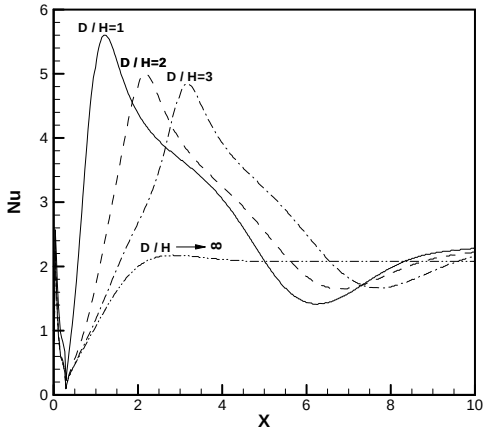

a) Distribution of Nusselt number along the bottom wall

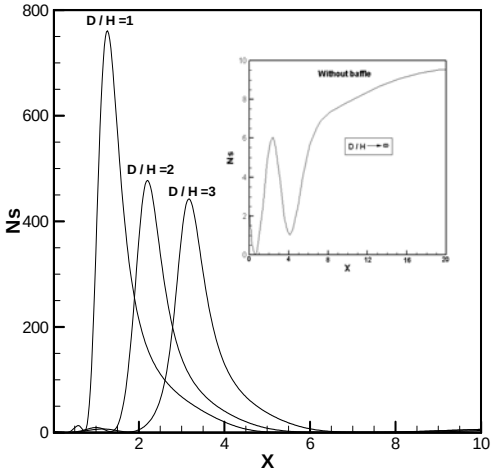

b) Distribution of entropy generation number along the bottom wall

Fig. 10. Effect of baffle on the distributions of Nusselt number and entropy generation number along the bottom wall (without bleeding)

Variations of entropy generation number along the bottom wall at different locations of baffle are demonstrated in Fig.10b. Also, the *Ns* variation in BFS flow without baffle is plotted in another coordinate system in this figure because of different orders in the values of *Ns*. Figure 10b shows that the baffle makes a different trend in *Ns* distribution along the bottom wall in comparison to BFS flow without baffle. In the absence of baffle, the value of entropy generation number decreases along the step length and reaches zero on the bottom wall at the step corner. After this point, *Ns* increases and the maximum value

of *Ns* occurs inside the recirculation zone and then drops sharply to a very low value at the reattachment point after which *Ns* increases and approaches to a constant value far from the step. However, the presence of baffle causes a different trend for entropy generation number such that the baffle effect dominates entropy generation. According to Fig. 10b, the maximum entropy generation number occurs on the bottom wall just below the baffle. Also, a considerable increase in the value of maximum entropy generation number is seen because of the baffle. For example, in the case of D/H=1, the maximum entropy generation number is about 80 times for $D/H \to \infty$ (without baffle). This is related to the increased temperature and velocity gradients below the baffle where the flow is directed towards the bottom wall. Also, it is seen that the value of maximum entropy generation number increases as the baffle moves toward the BFS.

The average Nusselt number along the heated wall is a good parameter for comparing the effects of these two methods on enhancing convection heat transfer. For this purpose, the variations of average Nusselt number with Re in the cases of employing suction and using baffle are shown in Fig. 11. It is seen that both of these methods increase the convection coefficient, such that using baffle has a slightly greater effect on average Nusselt number along the heated wall. Moreover, it is seen that convection coefficient has increasing trend with Reynolds number.

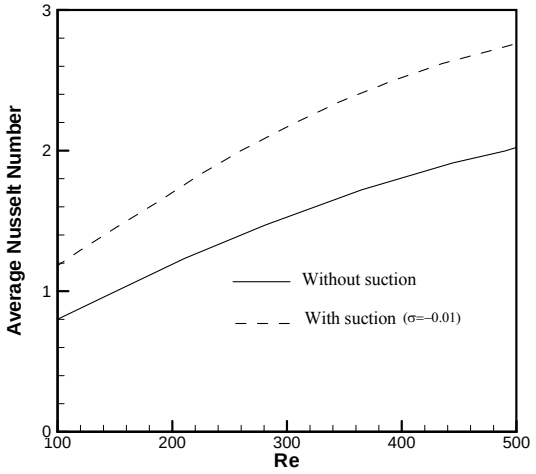

a) Effect of suction on average Nu

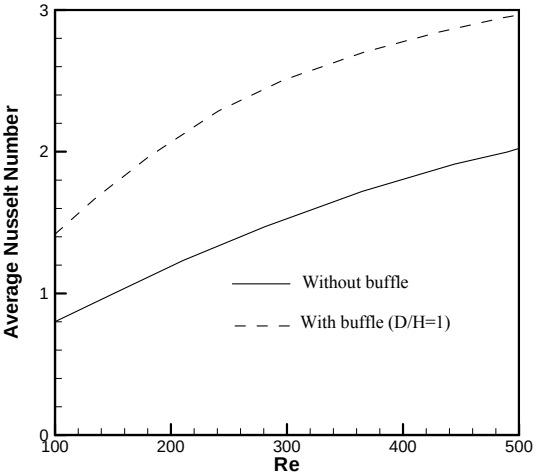

b) Effect of baffle on average Nu

Fig. 11. Variation of the average Nusselt number with *Re*

Finally, to compare the performances of these two methods (using baffle and suction) in enhancing the convection heat transfer by the second law analysis, the amount of total entropy generation inside the

whole flow domain in the range of $0 \le x \le 20H$ is calculated and results are shown in Figs. 12 and 13. It should be mentioned that the value of total entropy generation in a convection flow can show the amount of irreversibilities that take place by both heat transfer and friction. As it is depicted in these figures, the total entropy generation number inside the flow domain increases with increase in *Re*, especially in the cases of employing suction with high bleeding coefficient or installing baffles near the step. But it is seen that the amount of irreversibilitiy because of the baffle is much higher than that for the suction process, although in enhancing the convection heat transfer, these two methods have almost equal effects.

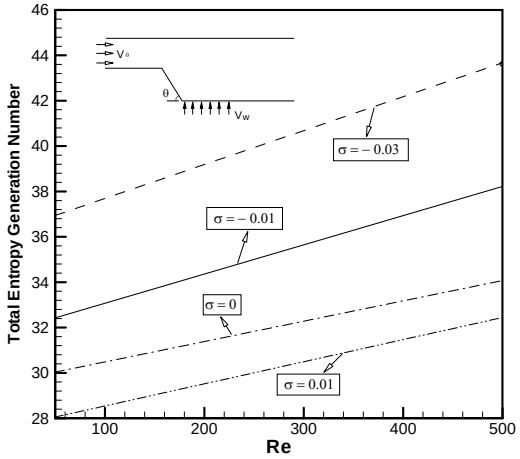

Fig. 12. Variation of the total entropy generation number with *Re* at different bleeding coefficient (without baffle)

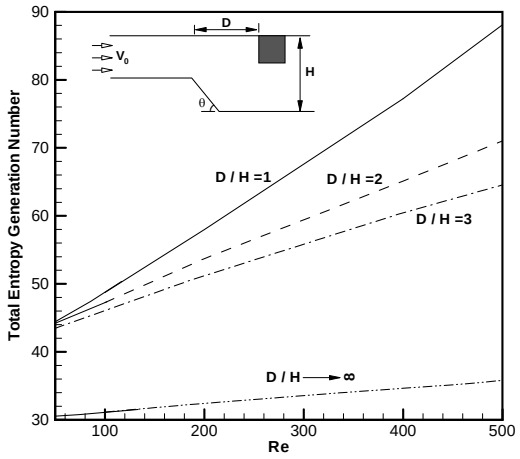

Fig. 13. Variation of the total entropy generation number with *Re* at different baffle location (without bleeding)

5. CONCLUDING REMARKS

The present research is focused on second law analysis of laminar convection over an inclined backward facing step to examine two different methods for enhancing heat transfer. Entropy generation in the flow domain due to the viscous effect and heat transfer is calculated numerically under bleeding condition using suction/bowing and also under the presence of wall mounted baffles. The set of governing equations for the fluid flow, heat transfer and entropy generation are solved numerically by CFD techniques. By this numerical approach, entropy generation due to separation, reattachment, recirculation and heat transfer is studied for flow over inclined step in a duct. The main results obtained in the present study are summarized as follows:

1- In the convection flow over BFS, the minimum value of entropy generation number along the bottom wall occurs at the step corner, where the fluid has no motion, and the maximum value of *Ns* takes place inside the recirculation zone and then drops sharply to a very low value at the reattachment point.
2- About the distribution of convection heat transfer coefficient along the bottom wall, numerical results revealed that the minimum value of Nusselt number occurs at the step corner and the maximum value at the reattachment point.
3- It was found that both employing suction and using baffle enhance the heat transfer, but the latter method produces large irreversibilities compared to the former.

Finally, it should be mentioned that the laminar and two-dimensional simplifying assumptions considered in the present work are the main limitations that will be resolved in future works by the authors. Also, it is worth mentioning that the numerical results about entropy generation obtained in this research work can be used by other investigators by applying second law analysis in designing thermal systems with less irreversibility in optimum condition.

NOMENCLATURE

a	distance between inlet section and step (m)
b	duct height before the step (m)
Br	Brinkman number
c	heat capacity (kJ/kg K)
D_H	hydraulic diameter =2b (m)
D	distance between the baffle and step (m)
ER	expansion ratio (H/b)
H	channel height after the step (m)
h	convection coefficient ($W.m^{-2}.K^{-1}$)
h_b	baffle's height (m)
k	thermal conductivity ($W.m^{-1}.K^{-1}$)
L	length of the channel after the step (m)
L_b	length of permeable wall with suction or blowing (m)
Ns	entropy generation number
Nu	Nusselt number
P	dimensionless pressure
p	pressure (Pa)
Pr	Prandtl number
Re	Reynolds number
s''_{gen}	entropy generation per unit volume $(W.m^{-3}.K^{-1})$
S_Φ	source term
T	temperature (K)
(u, v)	x- and y- velocity components (m / s)
(U, V)	nondimensional velocity components
V_0	fluid velocity at inlet section (m / s)
$\forall$	volume of computational domain
w_b	baffle's width (m)
(x, y)	coordinates in physical plane (m)
(X, Y)	dimensionless forms of (x, y)

Greek Symbols

θ	step inclined angle
Θ	non-dimensional temperature
σ	bleed coefficient , v_w/V_0
ρ	density $(kg.m^{-3})$
μ	dynamic viscosity $(kg\ m^{-1}s^{-1})$
Ψ	viscous dissipation number
τ	dimensionless temperature parameter
ϕ	viscous dissipation
Φ	dependent variable

Subscripts

b	baffle
c	cold wall
cond	conduction
h	hot wall
i	inlet
r	reattachment
visc	viscous
N,S,E,W	north, south, east and west
w	wall

REFERENCES

1. Bejan, A. (1982). *Entropy generation through heat and fluid flow*. Wiley, New York.

2. Ko, T. H. & Wu, C. P. (2009). A numerical study on entropy generation induced by turbulent forced convection in curved rectangular ducts with various aspect ratios. *International Communications in Heat and Mass Transfer*, Vol. 36, pp. 25-31.
3. Bahrami, A. & Gandjalikhan Nassab, S. A. (2010). Study of entropy generation in laminar forced convection flow over a forward-facing step in a duct. *International Review of Mechanical Engineering*, Vol. 4, No. 4, pp. 399-404.
4. Abu Nada, E. (2005). Numerical prediction of entropy generation in separated flows. *Entropy*, Vol. 7, No. 4, pp. 234-252.
5. Abu Nada, E. (2006). Entropy generation due to heat and fluid flow in backward-facing step flow with various expansion ratios. *International Journal of Exergy*, Vol. 3, No. 4, pp. 419-435.
6. Duwez, P. & Wheeler, H. L. (1948). Experimental study on cooling by injection of fluid through porous material. *Journal of Institution of Aero Science*, Vol. 15, pp. 509-521.
7. Mehta K. N. & Jain, R. K. (1962). Laminar hydrodynamic flow in a rectangular channel with porous walls. *Proc. Nat. Inst. Sci. India*, Vol. 28, pp. 846–856.
8. Erdogan, M. E. & Imrak, C. E. (2005). On the axial flow of an incompressible viscous fluid in a pipe with a porous boundary. *Acta Mech*., Vol. 178, pp. 187–197.
9. Abu Nada, E. (2009). Investigation of entropy generation over a backward-facing step under bleeding conditions. *Energy Conversion and Management*, Vol. 49, pp. 3237-3242.
10. Atashafrooz, M. & Gandjalikhan Nassab, S. A. (2013). Simulation of laminar mixed convection recess flow combined with radiating heat transfer. *Iranian Journal Science & Technology, Transaction of Mechanical Engineering*, Vol. 37, No. M1, pp. 71-75.
11. Tsay, Y. L., Chang, T. S. & Cheng, J. C. (2005). Heat transfer enhancement of backward-facing step flow in a channel by using baffle installation on the channel wall. *Acta Mechanica*, Vol. 174, No. 1-2, pp. 63- 76.
12. Nie, J. H., Chen, Y. T. & Hsieh, H. T. (2009). Effects of a baffle on separated convection flow adjacent to backward-facing step. *International Journal of Thermal Sciences*, Vol. 48, pp. 618-625.
13. Patankar, S. V. & Spalding, B. D. (1972). A calculation procedure for heat, mass and momentum transfer in three-dimensional parabolic flow. *International Journal of Heat Mass Transfer*, Vol. 15, pp. 1787-1806.
14. Armaly, B. F., Durst, F., Pereira, J. C. F. & Schonung, B. (1983). Experimental and theoretical investigation of backward-facing step flow. *J. Fluid Mechanics*, Vol. 127, pp. 473-496.